

## **Electronic supplementary information (ESI)**

### **Fast carbonylation reaction from CO<sub>2</sub> using plasma gas/liquid microreactors for radiolabelling applications**

Marion Gaudeau<sup>a</sup>, Mengxue Zhang<sup>a</sup>, Michael Tatoulian<sup>a</sup>, Camille Lescot<sup>b\*</sup>, Stéphanie Ognier<sup>a\*</sup>

<sup>a</sup> Chimie ParisTech-PSL, PSL Université Paris, CNRS, Institut de Recherche de Chimie Paris, UMR 8247, 2PM Group, 11 rue Pierre et Marie Curie, 75005 Paris, France.

<sup>b</sup> Chimie ParisTech-PSL, PSL Université Paris, CNRS, iCLeHS, FRE 2027, SEISAD Group, 11 rue Pierre et Marie Curie, 75005 Paris, France.

\* Corresponding authors : [stephanie.ognier@chimieparistech.psl.eu](mailto:stephanie.ognier@chimieparistech.psl.eu) ;  
[camille.lescot@chimieparistech.psl.eu](mailto:camille.lescot@chimieparistech.psl.eu)

## Table of content

Preparation of the plasma microreactor .....	3
Lithography .....	3
Sputtering .....	3
Lift-off.....	3
Power assessment .....	5
Reaction in batch process .....	7
Calculation details concerning the study of the CO volume concentration in the gas phase .....	8
Calculation details concerning the influence of the liquid residence time in equimolar conditions .....	9
CO pressure calculation .....	10
<sup>1</sup> H NMR analysis and conversion calculation method .....	12
References .....	15

## Preparation of the plasma microreactor

Copper electrodes having a comb shape were deposited by the sputtering technique described thereafter on the outer side of the glass microreactor. The different steps of electrodes deposition are shown in Figure S1. The teeth of this comb are positioned at the walls of the canals, allowing visual access to the canals despite the opacity of the metal.

### Lithography

In order to deposit patterned electrodes, we used photolithography techniques. Microposit S1818 photosensitive resin (Rohm and Haas Company, US) was coated by spin-coating (3500 rpm, 30 s) on the surface of the glass microreactor to form a 0.5  $\mu\text{m}$  photoresist layer. A photomask was produced from a plastic film coated with a photosensitive layer, with a high-resolution laser photoplotter, reproducing transparent/opaque patterns according to the electrode design. The microreactor covered with photoresist was then exposed to 250  $\text{mJ}\cdot\text{cm}^{-2}$  of UV radiation at 365 nm through this photomask in a UV-KUB exposure device (KLOÉ, France), before being developed in the Microposit MF-319 developer. After thorough cleaning and drying, a patterned thin film photoresist was deposited on the glass reactor.

### Sputtering

The copper electrodes were then deposited by magnetron sputtering, in a hybrid reactor (HSPT520, Plasmionique Inc, Canada). The reactor was mounted on the sample holder and kept at 30 cm from the Cu target. After a first step of plasma cleaning with Ar/O<sub>2</sub>, the deposition was realized under Argon atmosphere with a plasma power of 100 W during 20 min.

### Lift-off

Finally, an acetone bath dissolved the remaining resin, removing the metallic deposits on its surface. The remaining copper deposit fixed on the glass therefore ultimately has the form provided by the photomask. The microreactor with the deposited comb-shaped copper electrode is shown in Figure S2a.

These three first steps (lithography, sputtering and lift-off) were repeated for the other side of the microreactor.

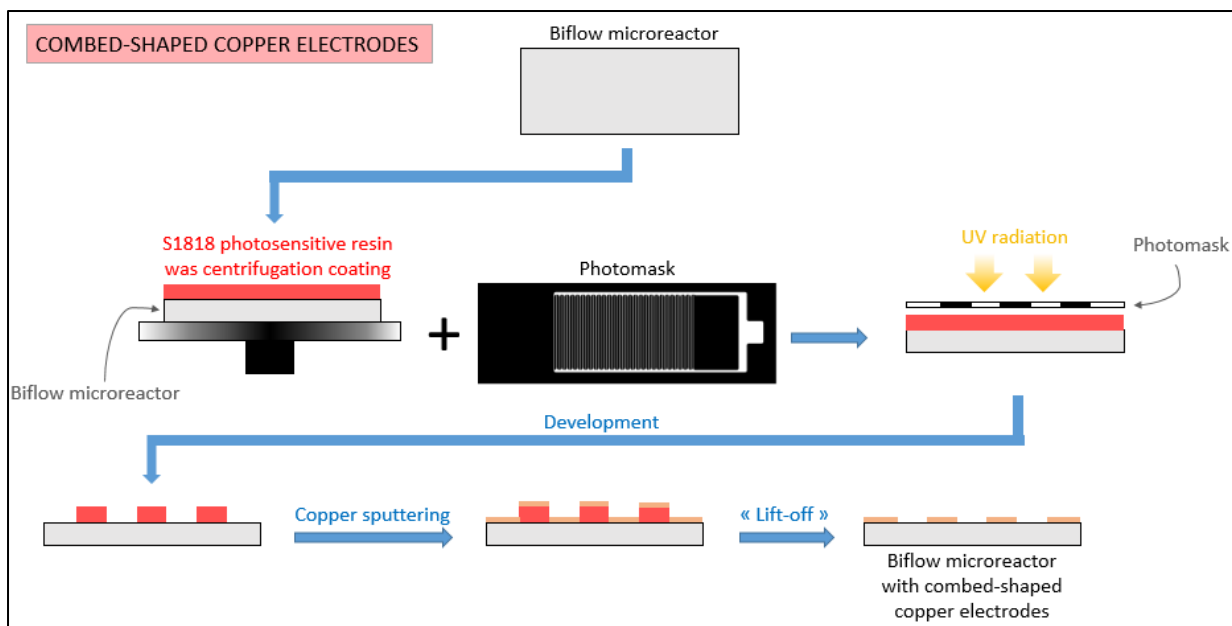


Figure S1: Steps for depositing copper electrodes on the microreactor

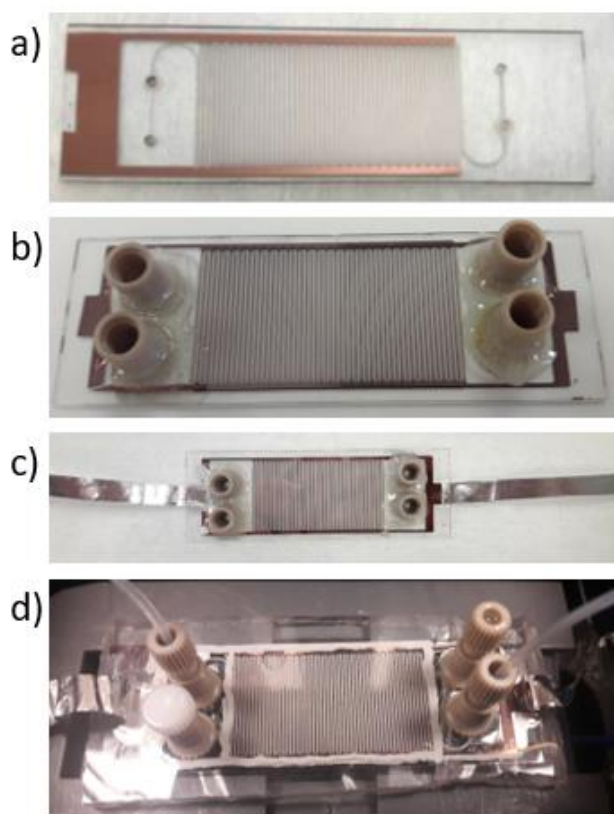


Figure S2 : a) Comb-shaped copper electrode deposited on one side of a glass microreactor; b) Microreactor with electrodes deposited on each side and nanoports; c) With aluminium foil connected to copper electrodes by means of silver paint; d) With PDMS coating

## Power assessment

Electrical measurements were obtained using an oscilloscope (PicoScope 5000 Series) to record the operating voltage  $U_{total}$  across the microreactor plus the capacitor through the 1000:1 outlet of the amplifier, and the voltage  $U_C$  across the capacitor measured by a low voltage probe (Teledyne LeCroy PP024 500 MHz 10:1). The operating voltage  $U_{total}$  is generated by a low frequency generator (ELC, GF467F, 5MHz) to a voltage amplifier (TREK 10/40A high voltage amplifier  $\times 1000$ ).

The measurement of the electrical power supplied to the microreactor was determined using the Lissajous method<sup>1-3</sup>. The Lissajous figure is obtained by plotting the charge flowing into the microreactor  $q$  as a function of the voltage difference  $U_R$  between the electrodes of the microreactor. The charge  $q$  is measured by means of the capacitor in series with the microreactor, inserted between the reactor and the ground; and  $U_R$  was the difference between  $U_{total}$  and  $U_C$ . The capacitor  $C_C$  was chosen sufficiently large (around 100 times bigger than the microreactor capacitance) so that the voltage difference  $U_R$  between the DBD electrodes was almost equal to the voltage  $U_{total}$  applied to the couple “microreactor + capacitor”. In this study, the capacitance of the reactor was 31.5 pF and the capacitor used was 3.11 nF.

When the imposed electric field is too small for plasma generation,  $U_C$  versus  $U_{total}$  plot is a straight line, because the system behaves as a purely capacitive cell and the charge varies proportionally to the voltage. Otherwise, if the voltage amplitude is high enough for discharge ignition, the Lissajous plot takes the form of a parallelogram. The area enclosed by the figure corresponds to the energy consumed per cycle of the operating voltage.

The voltage  $U_C$  across the capacitor is proportional to the charge  $q$  which has passed through the microreactor:

$$dU_C = \frac{1}{C_C} dq$$

It is thus possible to write the energy  $E$  transferred during a period:

$$E = \int U_R dq = C_C \int U_R dU_C = C_C \int (U_{total} - U_C) dU_C = A_{Lissajous}$$

Hence, the average power transferred to the microreactor is deduced by multiplying by the frequency.

$$P = f \times E$$

A Python program was written to calculate this power, averaged over a whole number of periods (generally between 5 and 10 periods according to the frequency used) from data retrieved from the oscilloscope ( $U_{total}$  and  $U_C$ ).

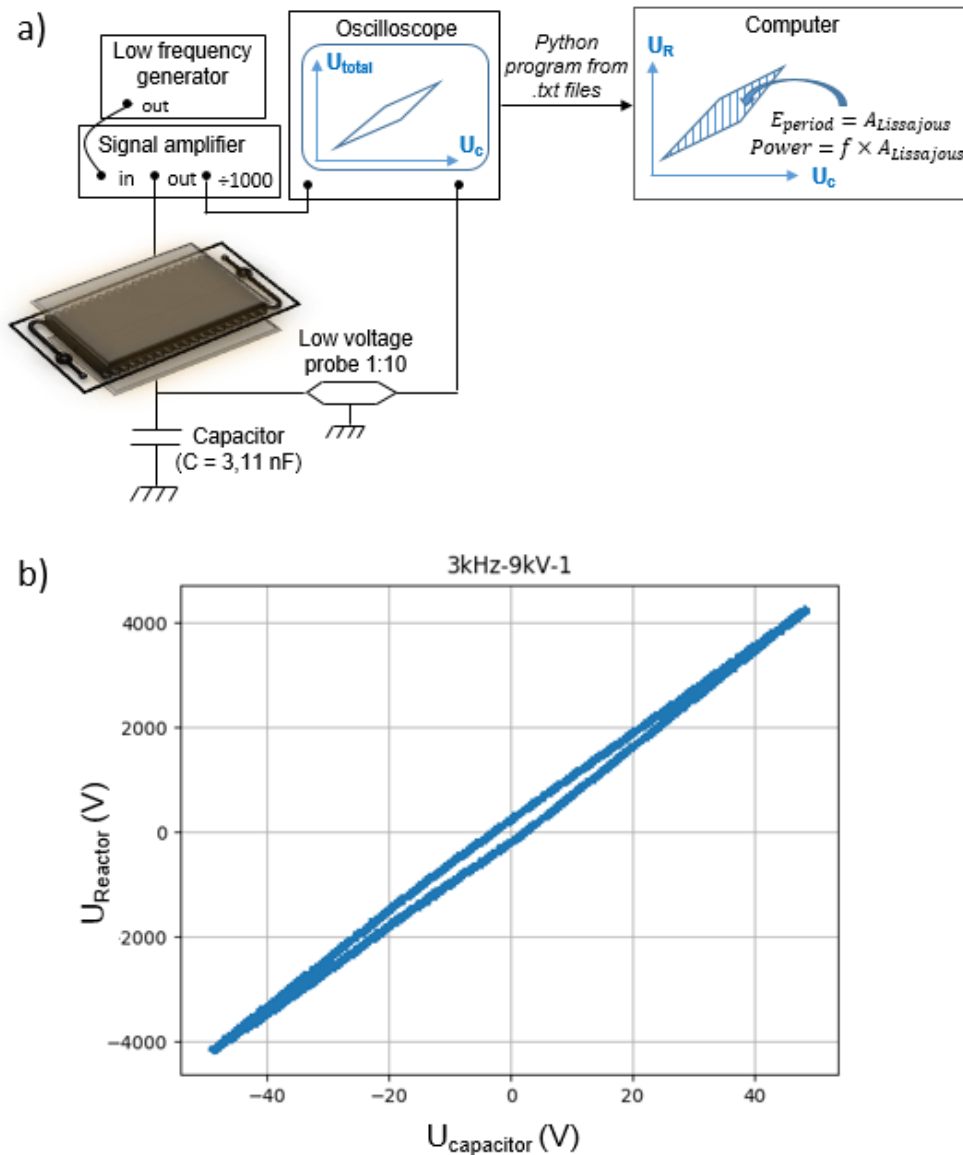


Figure S3: a) Diagram of the power discharge calculation method principle from Lissajous figure; b) Lissajous figure obtained from Python program for Ar:CO<sub>2</sub> 90:10 at 3 kHz and 9 kVpp

## Reaction in batch process

The aminocarbonylation reaction has been done in batch process to compare with the microfluidic process at the optimal temperature (50 °C). Solid raw materials were first added to a 25 mL round bottom flask:

- 7.2 mg (= 0.0125 mmol = 5 %mol) of Bis(dibenzylideneacetone)palladium(0) (Pd(dba)<sub>2</sub>) (Aldrich)
- 6.6 mg (= 0.025 mmol = 10 %mol) of 4,5-Bis(diphenylphosphino)-9,9-dimethylxanthene (Xantphos) (Alfa Aesar 97%)
- 58.5 mg (0.25 mmol = 1eq) of 4-Iodoanisole (Aldrich 98%)

Then, liquid raw materials were added to the 25 mL round bottom flask:

- 3 mL of Dioxane (VWR ≥99% stabilised with BHT 25 ppm)
- 65.7 μL (= 0.5 mmol = 2 eq) of n-hexylamine (Aldrich 99%)
- 69.7 μL (0.5 mmol = 2 eq) of trimethylamine (Alfa Aesar ≥99%)

It corresponds to the same concentrations as in microfluidics process. The flask was closed with a septum and a balloon filled of CO was needled through it. The reaction was carried out during 45 min at 50°C with a magnetic stirrer.

## Calculation details concerning the study of the CO volume concentration in the gas phase

With an optimized liquid flowrate of 15  $\mu\text{L}/\text{min}$ , and a substrate concentration of  $8.3 \times 10^{-8}$  mol/ $\mu\text{L}$  (0.25 mmol of substrate into 3 mL of dioxane),  $F_{\text{SUBSTRATE}}$  was equal to  $2.08 \times 10^{-8}$  mol/s.  $F_{\text{CO}}$  (mol/s) was deduced according the value of the ratio  $F_{\text{CO}}/F_{\text{SUBSTRATE}}$ . Then the CO flowrate was calculated by multiplying the gas perfect molar volume (22.4 L/mol) by  $F_{\text{CO}}$  :

$$Q_{\text{CO}} (\text{mL}/\text{min}) = F_{\text{CO}} (\text{mol}/\text{s}) \times 22.4 (\text{L}/\text{mol}) \times 1000 \times 60$$

Then, CO was supplemented with argon to reach the optimized total flowrate of gas that has been previously found equal to 2.5 sccm.



## Calculation details concerning the influence of the liquid residence time in equimolar conditions

According to the liquid flowrate used (15, 10 and 7.5  $\mu\text{L}/\text{min}$ ),  $F_{\text{SUBSTRATE}}$  was calculated using substrate concentration of  $8.3 \times 10^{-8}$  mol/ $\mu\text{L}$  (0.25 mmol of substrate into 3 mL of dioxane) :

$$F_{\text{SUBSTRATE}} = \frac{Q_{\text{liq}} (\mu\text{L}/\text{min})}{60} \times 8.3 \cdot 10^{-8} (\text{mol}/\mu\text{L})$$

Then, since  $F_{\text{CO}}/F_{\text{SUBSTRATE}}$  was equal to 1,  $F_{\text{CO}}$  (mol/s) was deduced. Then the CO flowrate was calculated by multiplying the gas perfect molar volume (22.4 L/mol) by  $F_{\text{CO}}$  :

$$Q_{\text{CO}} (\text{mL}/\text{min}) = F_{\text{CO}} (\text{mol}/\text{s}) \times 22.4 (\text{L}/\text{mol}) \times 1000 \times 60$$

Then, CO was supplemented with argon to reach the total flowrate of gas that has been defined to maintain a gas-liquid hydrodynamic equilibrium.

## CO pressure calculation

The total gas pressure at the inlet of the microreactor, depending on the flow rates of both gas and liquid phase, was measured using the setup demonstrated in Figure S5. A stable flow of Ar-Cyclohexane was studied.

The gas pressure was imposed using a Fluigent pressure controller, and the gas flowrate was measured with a mass flow controller (Bronkhorst), placed between the pressure controller and the microreactor, with its valve fully open. The flowrate was verified using a bubble flow meter placed at the outlet of the reactor. Figure S6 plots the relation between the gas flowrate and the gas total pressure, at various liquid flowrates.

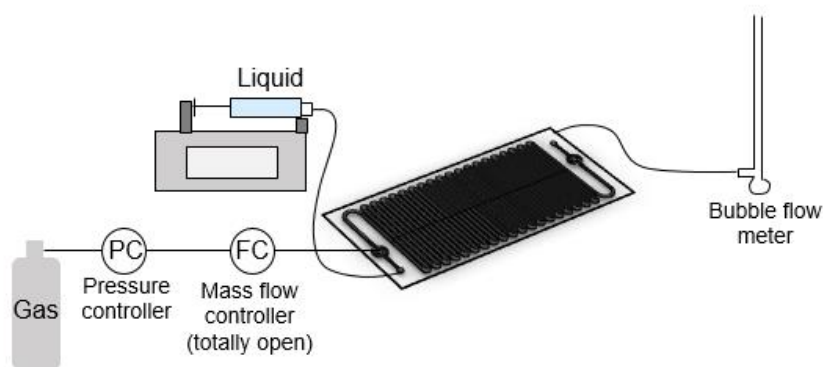


Figure S4: Diagram of the experimental set up for gas inlet pressure measurements

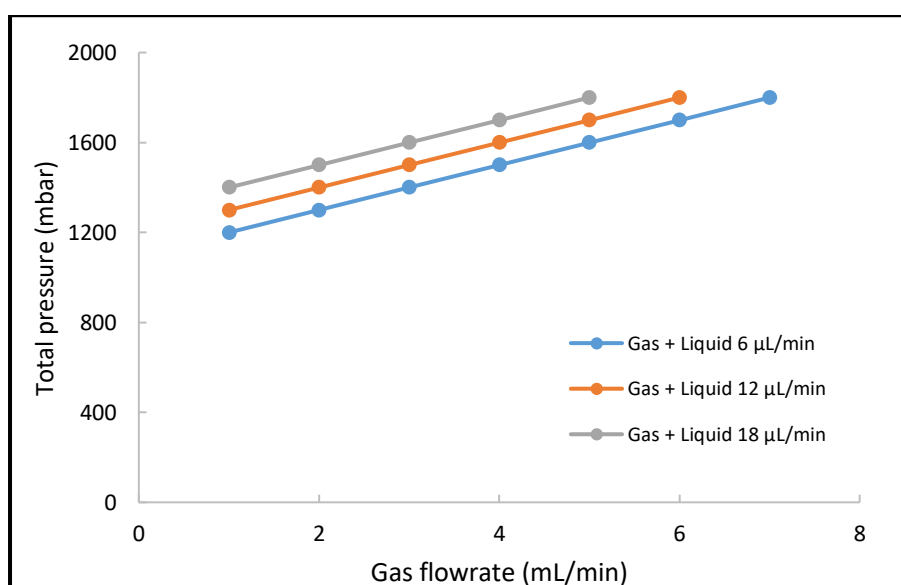


Figure S5: Graph of the inlet gas pressure as a function of the inlet gas flowrate at ambient temperature

For our study, we have assumed that the type of liquid had no influence on the measure of pressure. Linear regressions have been done to calculate the total gas pressure at the inlet of the microreactor for a certain liquid flowrate.

## **<sup>1</sup>H NMR analysis and conversion calculation method**

Conversion of p-iodoanisole into the amide **1** was calculated by comparing the area of the peak of methoxy group of amide **1** to the area of the peak of methoxy group of the remained p-iodoanisole (Figure S7).

For that, the peak of methoxy group of amide **1** was first calibrated to 3, corresponding to the proton number of the methoxy group. Then the area of the peak of methoxy group of the remained p-iodoanisole was measured from this calibration, and the conversion was calculated according to the formula:

Substrate conversion (%)

$$= \frac{\text{area of the peak of methoxy group of amide } \mathbf{1} \text{ (at 3.81 ppm)}}{\text{area of the peak of methoxy group of amide } \mathbf{1} \text{ (at 3.81 ppm)} + \text{area of the peak of methoxy group of p - iodoanisole (at 3.75 ppm)}}$$

Figure S7 below is a <sup>1</sup>H NMR spectra of crude product, with explanation of the conversion calculation.

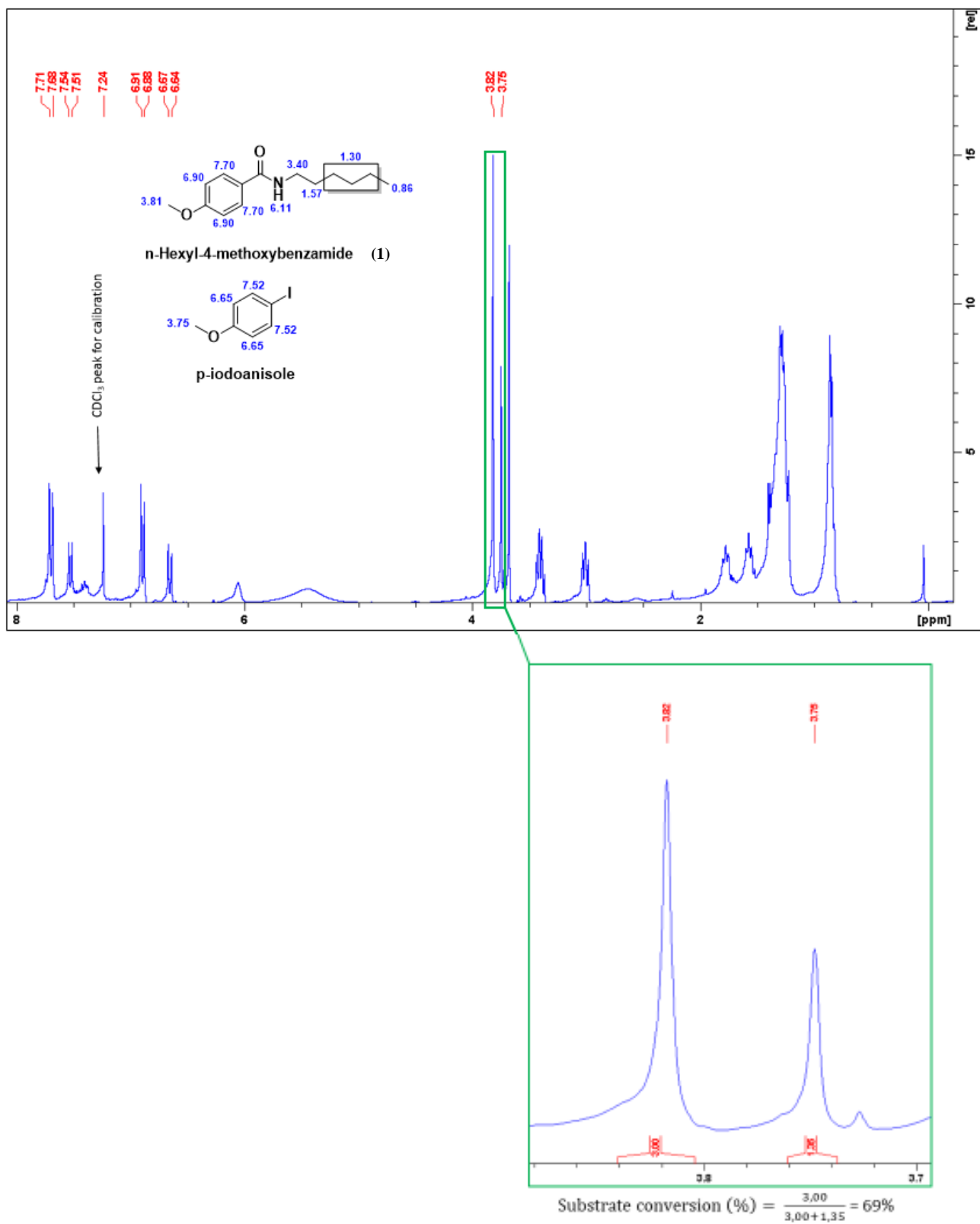


Figure S6 : NMR spectra of a crude product and conversion calculation principle

Figure S8 below represents the proton NMR spectra of the pure product after purification by chromatography on a silica column with an isolated yield of 95%

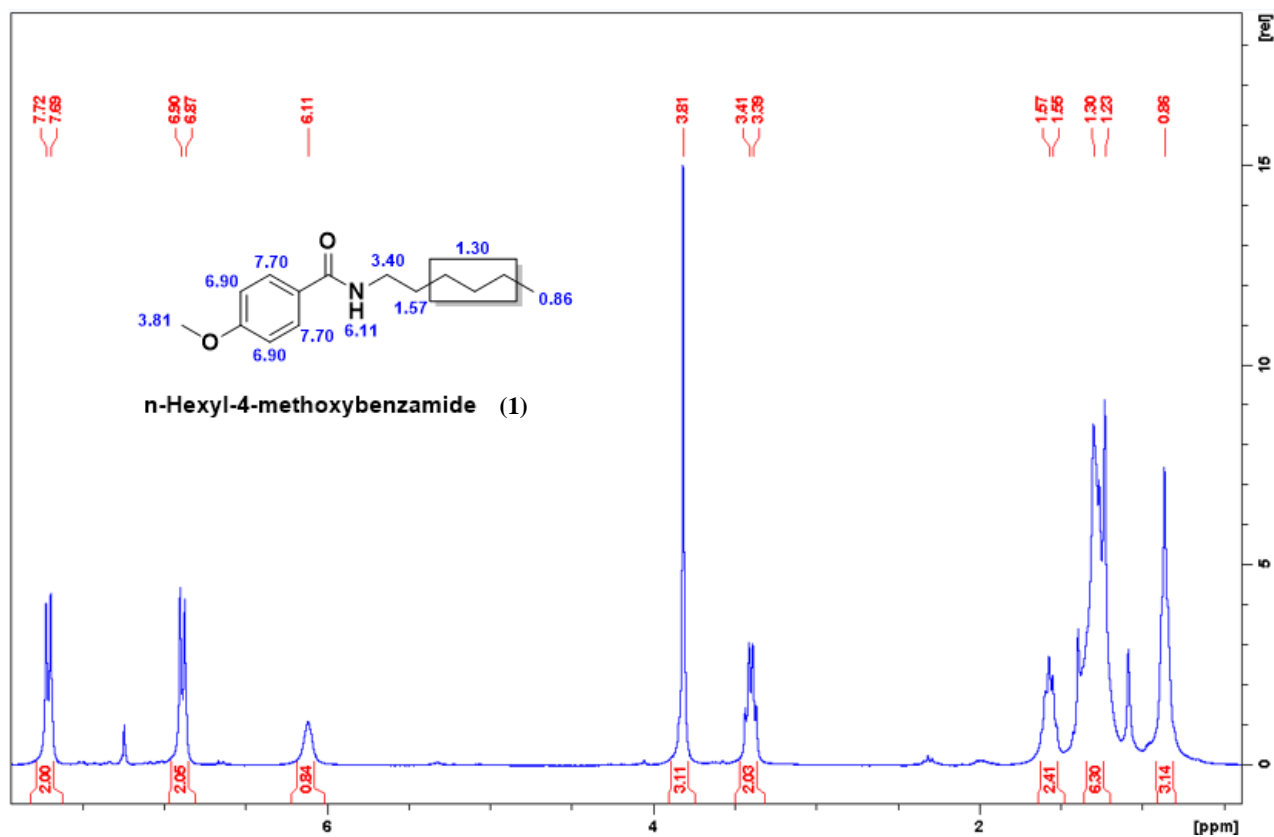


Figure S8 : NMR spectra of the pure amide (2) product

*n*-Hexyl-4-methoxybenzamide (**1**) :

$^1\text{H}$  NMR (400 MHz,  $\text{CDCl}_3$ )  $\delta$  7.70 (d,  $J = 9$  Hz, 2H), 6.90 (d,  $J = 9$  Hz, 2H), 6.11 (bs, 1H), 3.81 (s, 3H), 3.40 (m, 2H), 1.57 (m, 2H), 1.30-1.23 (m, 6H), 0.86 (m, 2H).

## References

- 1 J. Kriegseis, S. Grundmann and C. Tropea, *J. Appl. Phys.*, 2011, **110**, 013305.
- 2 I. Biganzoli, R. Barni, A. Gurioli, R. Pertile and C. Riccardi, *J. Phys. Conf. Ser.*, 2014, **550**, 012039.
- 3 J. Kriegseis, B. Möller, S. Grundmann and C. Tropea, *J. Electrostat.*, 2011, **69**, 302–312.